OPTIMIZATION OF DISPERSION COMPENSATION FOR LONG DISTANCE 40 Gbit/s SOLITON TRANSMISSION LINES BY THE Q-MAP METHOD

K. SHIMOURA, I. YAMASHITA AND S. SEIKAI
Technical Research Center of the Kansai Electric Power Co., Inc.
3-11-20 Nakoji, Amagasaki, Hyogo 661-0974, Japan

Abstract. We investigate periodic dispersion compensated 40 Gbit/s soliton transmission lines by a numerical simulation and transmission experiment. We developed the simulation method for the optimization of these lines using Q-maps. The optimal dispersion compensation becomes a constant value of ±20 ps/nm in different compensation periods, because of the optimal strength of the dispersion management. In the experiment, we evaluated transmission performance in the parameters of signal wavelength, signal power, and the location of dispersion compensation elements. The location is quite important in the design of such lines. In the 640 km transmission experiment using 2-pieces of dispersion compensation fibers, we observed error-free transmission in the wavelength range of 1.2 nm in the optimally designed line. This line design is practical for the next generation of 40 Gbit/s based communication systems.

1. Introduction

The 10 Gbit/s transmission systems using dispersion-shifted fibers are commonly used in Japan. The RZ-based 40 Gbit/s systems are expected to be the next generation medium distance high capacity communication systems. In this region, fiber dispersion effects and fiber nonlinear effects become critical. Dispersion managed (DM) soliton is an attractive solution in this area. This scheme also can be applied for ultra-long distance communication [1]-[3].

The periodic dispersion compensated lines are modeled by uniform dispersion fibers and linear dispersion compensation elements. The anomalous dispersion fiber-based transmission line was proposed for reducing the Gordon-House jitter and soliton interactions without decreasing the signal power [4]. It was also reported that the initial frequency chirping enhances the power margin and dispersion tolerance [5]. On the other hand, normal dispersion fiber-based transmission lines also have good performances for soliton transmission [6].

We have shown numerically that two extremely stable transmission conditions exist in this scheme [7]. And at these conditions, the strength of the dispersion management becomes optimal to minimize the soliton interaction [8]. From this result, the dense (short-scale, continuous) dispersion management scheme is proposed for ultra high bit rate transmission systems [9]-[11]. In this paper, we show the numerical optimization method for the design of dispersion compensated 40 Gbit/s systems.

2. Q-map method

In the 40 Gbit/s system, the signal power becomes large and we must consider the nonlinear effect and the dispersion effect. We must optimize many parameters simultaneously for the design of dispersion-managed lines. Q-factor contour mapping (Q-map) is a practical method for this purpose [12]. Q-factor represents the signal-to-noise ratio at the receiver decision circuit in voltage or current unit, and requires $Q > 6$ for the BER of 10^{-9} [13]. Figure 1 shows the definition of Q-factor for RZ pulses. In the definition (a), only one pulse is considered and we can easily estimate the stability of the pulse in a short calculation time. The definition (b) is the ordinary Q-factor definition applied to NRZ systems. This definition can be applied to RZ systems with some modification of the receiver bandwidth. We used 1.4 times of the base band frequency in the simulations. This definition considers soliton interaction effects and jitter effects, and a relatively short bit pattern can be used because the interaction between adjacent pulses is dominant in soliton systems.

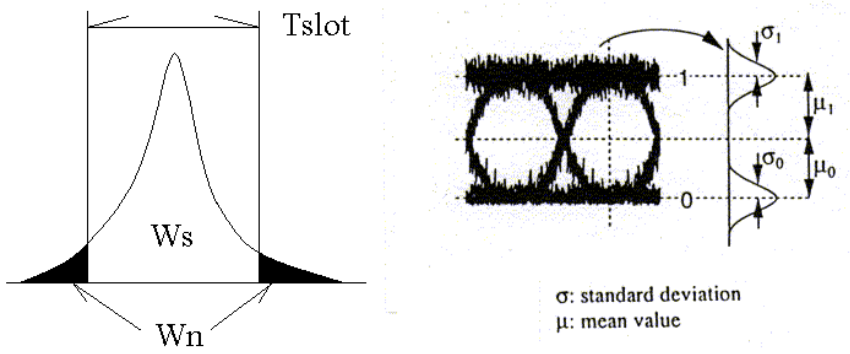

Figure 1. Q-factor definitions for RZ-pulses. (a) for one pulse stability analysis, and (b) for interaction and jitter analysis.

We proposed some kinds of Q-maps for the optimization of periodic dispersion compensated lines [7]. Figure 2 shows the dispersion maps of the simulation model. The dispersion-shifted fibers of dispersion *D* and length *La* are connected with optical amplifiers. A linear dispersion compensation element of *Dc* is installed in every *Nc* amplifier spans. *D* and *Dc* can be positive (anomalous) or negative (normal) values, and the average dispersion *Dav* is calculated from these values by the equation (1).

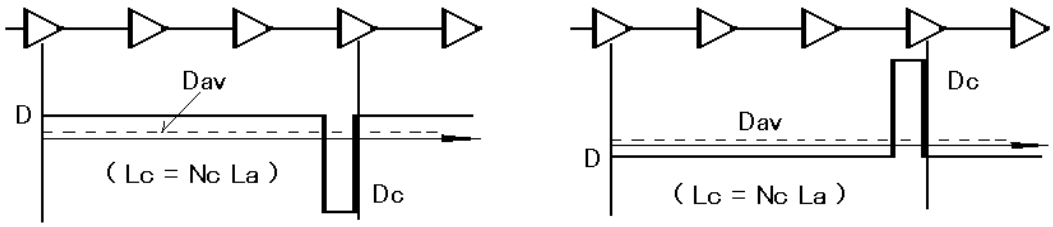

(a) Anomalous dispersion fiber based line (b) Normal dispersion fiber based line

Figure 2. Dispersion maps for the simulation analysis.

$$Dav = D + \frac{Dc}{Nc \cdot La} \tag{1}$$

The nonlinear Schrödinger equation (NLS), with a third order dispersion term of 0.07 ps/nm^2/km and a fiber attenuation term of 0.2 dB/km, is solved by the split step Fourier method. The factor 1/2 of the nonlinear operator *B* originates from the averaging of the electrical field over the cross section of the fiber [14]. The effective core area is 50 μm^2, and the Kerr coefficient is 2.24×10^{-20} m^2/W. The amplifier noise figure is 4 dB and a 6 nm width filter is used in each amplifier. We executed these calculations by the Mathematica 4.0 on the Windows NT operating system.

$$\frac{\partial}{\partial z}\phi = [\,A + B\,]\,\phi \qquad : \text{NLS}$$

$$A = -\frac{i}{2}\beta_2\frac{\partial^2}{\partial\tau^2} + \frac{1}{6}\beta_3\frac{\partial^3}{\partial\tau^3} - \frac{\alpha}{2} \qquad : \text{Linear}$$

$$B = \frac{i}{2}\gamma\left[\,|\phi|^2 - T_R\frac{\partial|\phi|^2}{\partial\tau}\,\right] \qquad : \text{Nonlinear}$$

$$\phi(0,\tau) = \sqrt{\frac{Pm}{S}}\exp\left[-\frac{\tau^2}{2T_0^2}(1-iC)\right]$$

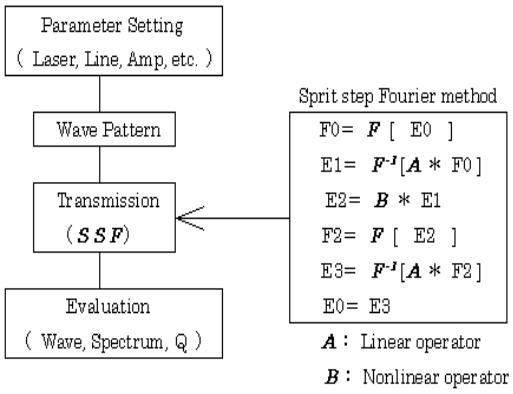

(a) Nonlinear Schrödinger equation (b) Split step Fourier method

Figure 3. (a) Nonlinear Schrödinger equation, and (b) Split step Fourier method. The chirped Gaussian pulse of chirp parameter *C* is assumed for the initial pulse.

3. Optimization of dispersion compensation

The chirped Gaussian pulse of 7.5-ps full-width at half-maximum (FWHM) is considered as the initial pulse and the 12-bit pattern "001011101100" is assumed. Figure 4 shows the example of the Q-maps on the *Dav* - *Dc* plane for the different compensation period *Nc*. The amplifier spacing *La* = 50 km, the initial peak power *Pm* = +13 dBm, and the transmission distance *Lt* = 3 Mm.

Two parameter zones are clearly demarcated for the stable transmission. One mode has a positive *Dc* value of around +20 ps/nm and the other mode has a negative value of around –20 ps/nm, and these values do not strictly depend on *Nc*. The positive *Dc* requires normal dispersion fibers as the transmission line, and negative *Dc* uses anomalous dispersion fibers. The optimal *Dav* is in the slightly anomalous region around +0.03 ps/nm/km in both cases. In *Nc* = 2 case (a), the local dispersions of the transmission fibers *D* are –0.17 ps/nm/km and +0.23 ps/nm/km, respectively. In *Nc* = 5 case (b), *D* is –0.05 ps/nm/km and +0.11 ps/nm/km, respectively. In the longer *Nc* case, the local dispersion becomes small, and nonlinear signal distortion effects become critical. The non-transmissible zone between transmissible zones is expanded and affected by the dispersion fluctuation of the transmission fiber. This effect determines the upper limit of the dispersion compensation period in higher bit-rate systems.

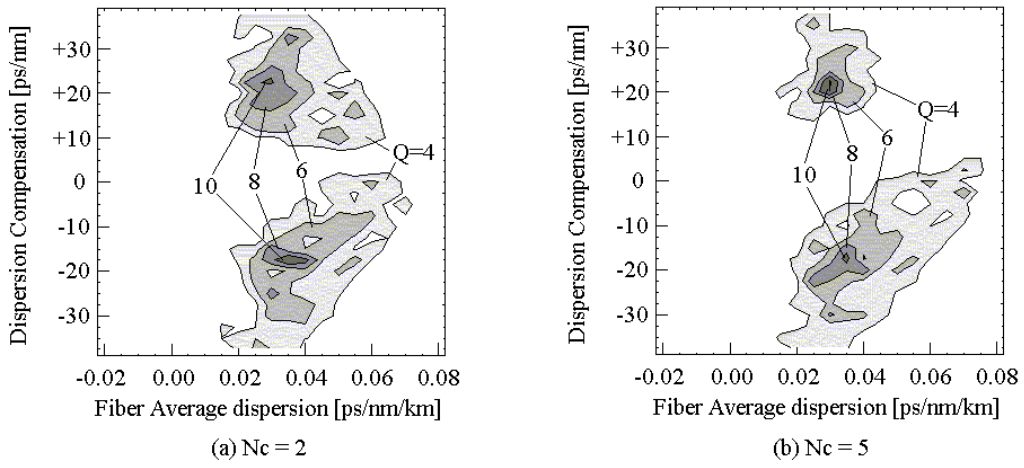

Figure 4. Q-maps on the *Dav* - *Dc* planes for different *Nc* cases. *Pm* = +13 dBm, *La* = 50 km and *Lt* = 3 Mm.

Figure 5 also shows the Q-maps on the *Dav* - *Dc* plane, but for different amplifier spacings. *La* = 30 km in case (a), and *La* = 80 km in case (b). The compensation period is *Nc* = 2 in both cases. In these cases, the optimal *Dc* is also about ±20 ps/nm, but the optimal *Dav* is slightly shifted. In the longer *La* case, the optimal *Dav* has a smaller value.

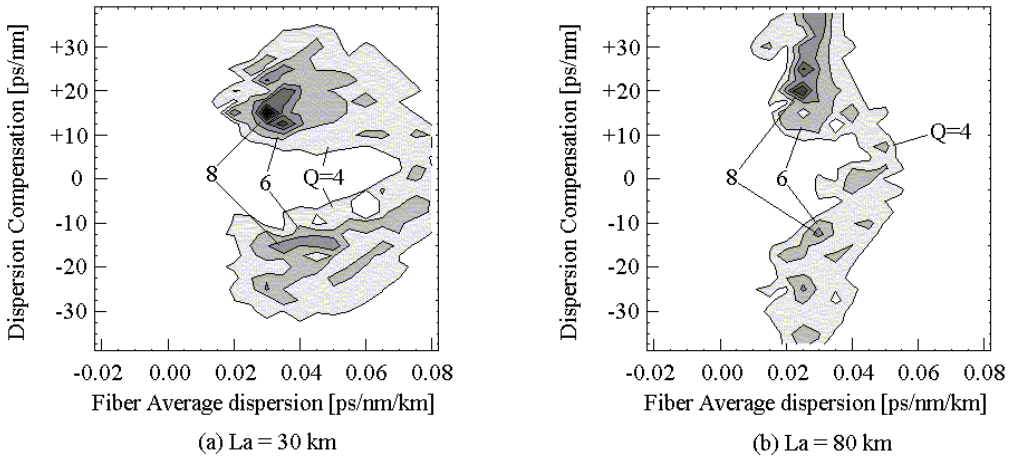

Figure 5. Q-maps on the *Dav* - *Dc* planes for different *La* cases. *Pm* = +13 dBm and *Nc* = 2.

Figure 6 shows the Q-maps on the *Dav* – *Pav* plane for a normal dispersion case (*Dc* = +20 ps/nm), and an anomalous dispersion case (*Dc* = –20 ps/nm). The amplifier spacing *La* = 50 km, and transmission distance *Lt* = 3 Mm. The fiber input power *Pav* is calculated from *Pm* by *Pav* = *Pm* – 8.0 dBm, considering the pulse duty ratio of 0.3 and the mark ratio of 0.5. The optimal *Dav* is about +0.04 ps/nm/km and the optimal *Pav* is about +6 dBm in both cases, but better transmission is achieved in the normal dispersion case (a). We can easily estimate the dispersion tolerance and the power margin of the transmissible area (Q > 6) and get,

$$Dav = +0.04 \pm 0.02 \text{ [ps/nm/km]} \quad (2a)$$

$$Pav = +6 \pm 2 \text{ [dBm]} \quad (2b)$$

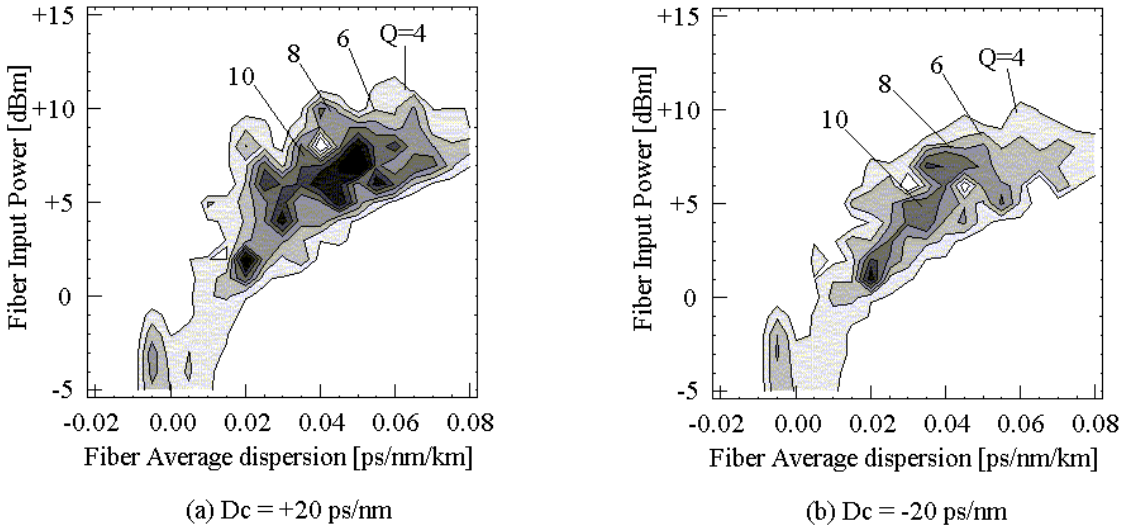

Figure 6. Q-maps on the *Dav* – *Pav* planes for normal dispersion case (*Dc* = +20 ps/nm) and anomalous dispersion case (*Dc* = -20 ps/nm).

4. The strength of the dispersion management

It is interesting that in the different *Nc* or *La* cases, the optimal dispersion compensation *Dc* has almost the same value. This means that the important parameter of the line design is not the local dispersion *D*, but the dispersion compensation *Dc*. These results are explained by the soliton interaction mechanism in the dispersion-managed lines. In the dispersion compensated line, the positive and the negative dispersions are almost cancelled, therefore the strength of dispersion management *S* is approximated by

$$S = \frac{\left| k_1 z_1 - k_2 z_2 \right|}{t_S^{\,2}} = 2.55 \frac{\left| Dc \right|}{T_S^{\,2}} \tag{3}$$

where $k = -(\lambda^2 / 2\pi c)\, d = 1.27\, D$ (ps/nm/km) for 1.55-μm range. *Ts* (ps) is the full-width at half maximum of the dispersion-managed soliton at the chirp-free point, and *Dc* (ps/nm) is the dispersion compensation value. Figure 7 indicates the pulse widths variations for a normal dispersion case (*Dc* = +20 ps/nm), and an anomalous dispersion case (*Dc* = –20 ps/nm) by the one-pulse transmission calculation. In the figure 7(a), the pulse width converges to the steady state by the guiding filter mechanism [15]. In the figure 7(b), the pulse width becomes minimal around the center point of the dispersion compensation spans, and *Ts* can be estimated from this point [16]. If we input *Dc* = ±20 ps/nm and *Ts* = 5.5 ps to the equation (3), we get *S* = 1.69. This value is almost same as the previous estimation of *S* = 1.65 [8].

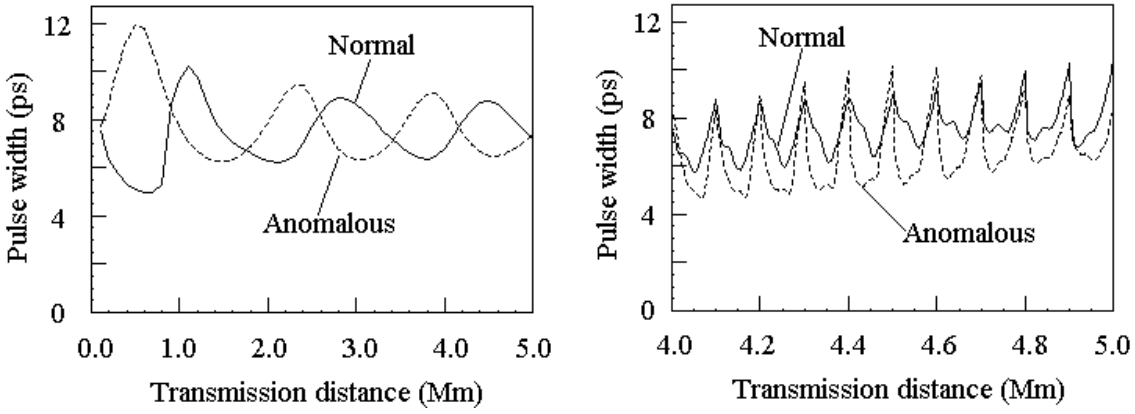

(a) Global pulse width (b) Local pulse width

Figure 7. Pulse widths in (a) global scale (every output point of compensation elements), and (b) fine scale. Normal case (*Dc* = +20 ps/nm) and Anomalous case (*Dc* = –20 ps/nm). *T* = 7.5 ps, *Pm* = +13 dBm, *Dav* = +0.03 ps/nm/km, *La* = 50 km and *Lc* = 100 km.

5. 40 Gbit/s soliton transmission experiment

40 Gbit/s based systems are considered to be the next generation high capacity medium distance communication systems [17, 18]. We evaluate experimentally the transmission performance of the 640 km single-channel straight-line systems in the parameters of signal wavelength, signal power, and the location of the dispersion compensation elements. We recognized the optimization of the location expands the wavelength tolerance remarkably without any initial frequency chirping.

The experimental setup is shown in the Figure 8. The optical pulse is generated by the mode-locked laser diode (MLLD), and the pulse width is 5.7 ps. This MLLD can be tuned between 1530 nm and 1560 nm wavelength range. The MLLD is triggered by 10 GHz clock. The output pulse is modulated by the lithium niobate modulator (LN-mod). The 10 Gbit/s, 2^{15}-1 PRBS data pattern is optically multiplexed to 40 Gbit/s signal by a PLC-multiplexer.

The dispersion-shifted fibers (DSF) are used as the transmission line. The amplifier spacing is 80 km consisting of 4-pieces of 20 km length DSF. The zero-dispersion wavelength of the each fiber is distributed between 1535 nm and 1560 nm, and their standard deviation is 6.1nm. The 2-pieces of dispersion compensation fibers (DCF) of –30 ps/nm and –40 ps/nm are installed in the transmission line. The averaged zero-dispersion wavelength is 1547.9 nm (without DCF), and 1549.5 nm (with DCF).

The amplifier noise Figure is 5 dB, and no-filter is used in each amplifier. The fiber loss rate is 0.21 dB/km, and the dispersion slope is 0.07 ps/nm^2/km. The average dispersion of the transmission line can be changed according to the laser-wavelength. In the receiver, 10 GHz clock signal is recovered by the 40 GHz phase locked loop circuit (PLL), and the 40 Gbit/s data stream is demultiplexed to 10 Gbit/s signal using an electroabsorbtion modulator (EA-mod).

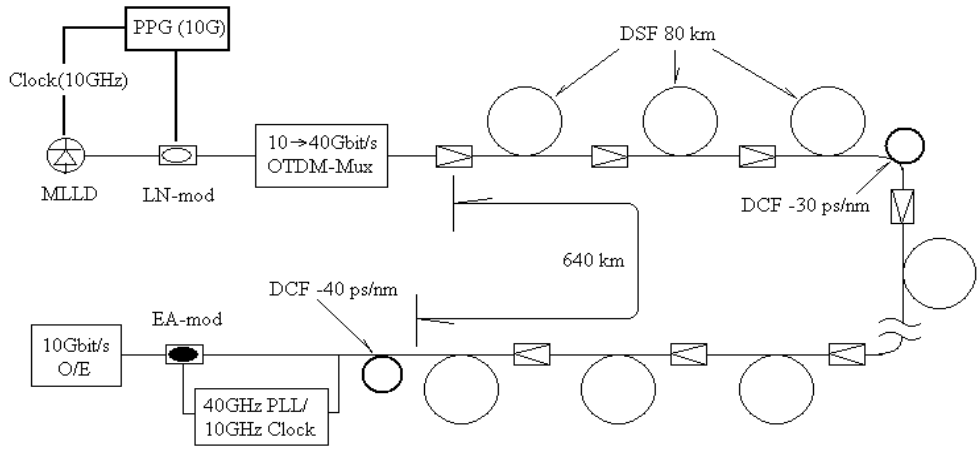

Figure 8. Experimental setup of the 40 Gbit/s, 640 km dispersion compensated transmission system using 2-pieces of DCF.

6. Optimization of the signal power

In dispersion compensated soliton systems, the optimal average dispersion is shifted nearly to zero and the power margins are expanded compared to the ordinary soliton systems [2, 4]. Figure 9(a) shows the signal power and the wavelength dependence of the transmission performance. The fiber input power is changed from +1 dBm to +9 dBm. The DCFs are installed in 320 km and 640 km points. The optimal amplifier output power is +7 dBm, and the good transmission BER < 10^{-9} is achieved between +3 dBm and +9 dBm. At +7dBm, the error free transmission is observed in the wavelength range of 0.4 nm: 1549.8 nm - 1550.2 nm, where the dispersion is +0.024 ps/nm/km to +0.052 ps/nm/km.

Figure 9(b) shows the estimation of the transmissible area by numerical simulation. This is a Q-map on the *Dav* – *Pav* plane, and requires Q > 6 for the BER less than 10^{-9} [12, 13]. From this Figure, the good transmission Q > 6 is achieved at the *Pav* from +1 dBm to +8 dBm, and the *Dav* from –0.01 ps/nm/km to +0.04 ps/nm/km. In this simulation, the dispersion fluctuation of the transmission fiber is not considered, and the fiber input power is estimated from the pulse peak power without considering the amplifier spontaneous emission (ASE) power. These two reasons will explain the difference between the experimental result and the simulation result.

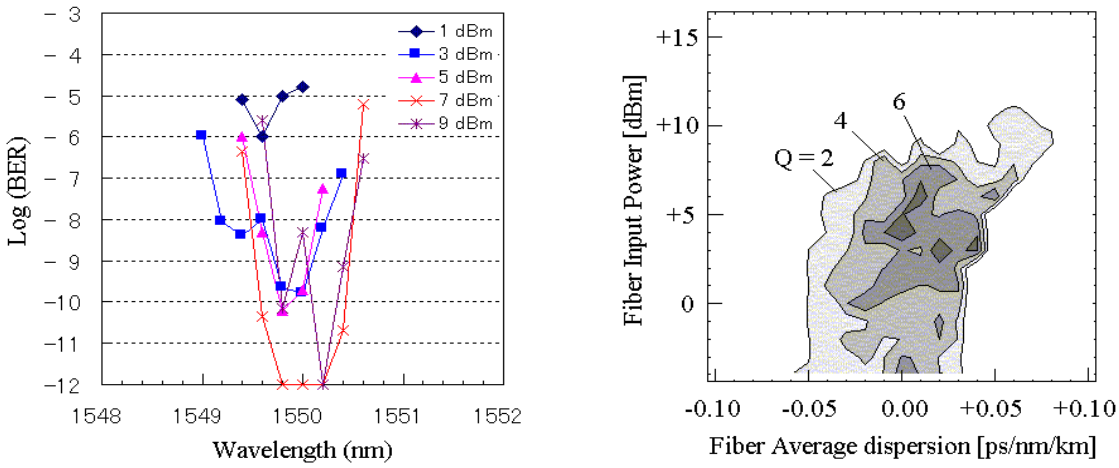

(a) Experiment (b) Simulation

Figure 9. Transmission dependence on the signal power (fiber input power) and the signal wavelength (average dispersion). (a) Experimental result and (b) Numerical simulation result.

7. Location effect of the dispersion compensation elements

In the dispersion compensated soliton systems, the pulse width becomes minimal around the center point of the dispersion compensation spans, where the frequency chirp becomes zero. Therefore, if we put the pulse source and the receiver at the chirp-free points, any pre-chirping or chirp compensation at the receiver is not required to get the optimal DM-soliton transmission.

Figure 10 shows the observed pulse widths in two types of dispersion compensation lines by the streak camera. In the case (a) the DCFs are installed in the end point of the compensation spans, 320 km and 640 km. In the case (b) these are installed in the center point of the spans, 160 km and 480 km. The average pulse widths at the receiver for 1549.2 nm to 1550.4 nm signals are 20.2 ps in the case (a), and 8.8 ps in the case (b). The pulse broadening is suppressed and intersymbol interference (ISI) is reduced in the case (b). Figure 11 shows the measured bit error rate for these two types of lines. In the case (b), the error-free transmission is observed in the wavelength range of 1.2 nm: 1549.4 nm - 1550.6 nm, expanded 3 times compared to the case (a).

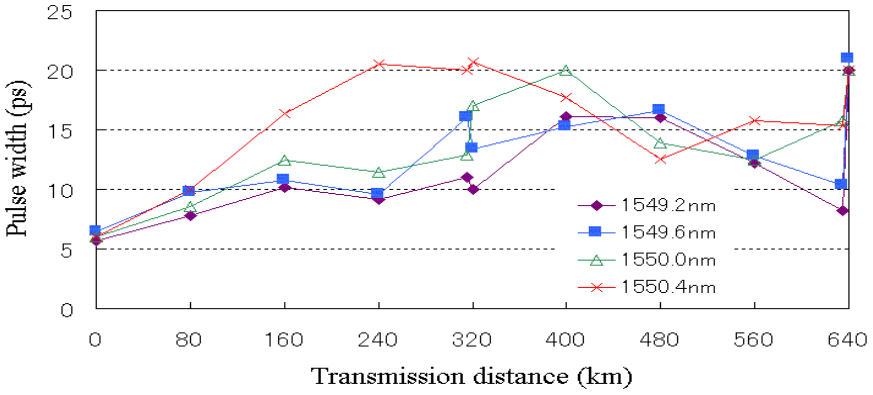

(a) Ordinary DCF allocation

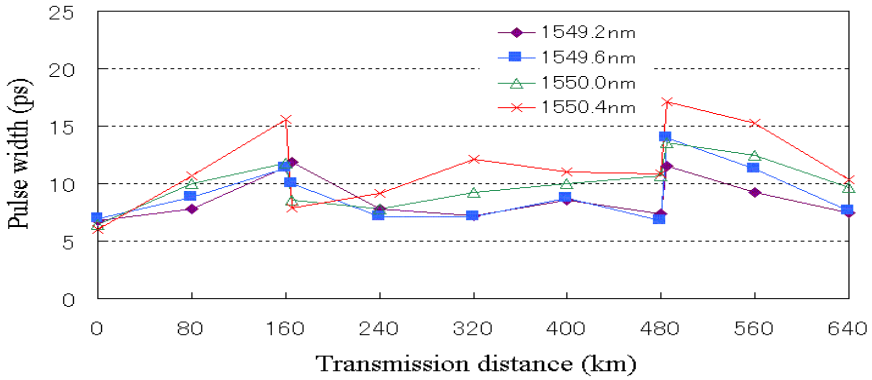

(b) Chirp-free DCF allocation

Figure 10. Pulse widths measured by a streak camera. DCFs are installed at the distance of (a) 320/640 km case and (b) 160/480 km case.

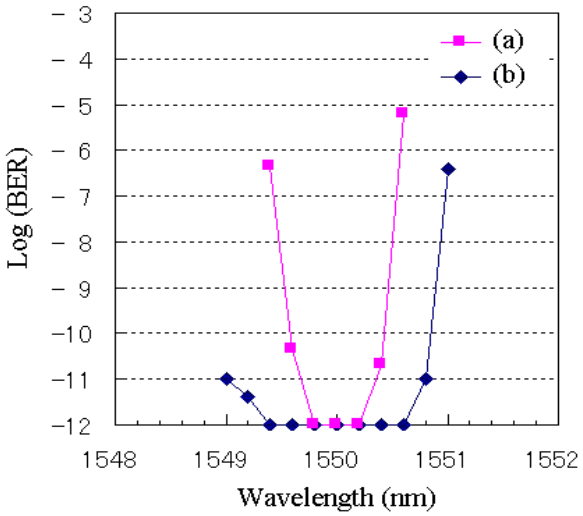

Figure 11. Transmission performance improvement by the location of DCFs.

Figure 12 shows the Q-maps on the initial frequency chirp parameter *C* and the dispersion compensation *Dc* plane. *Dav* is fixed to +0.03 ps/nm/km and *Pm* is +13 dBm. In the ordinary DCF allocation case (a), $C > 0$ (down-chirping) is required for the positive *Dc* lines, and $C < 0$ (up-chirping) is required for the negative *Dc* lines for the optimal transmission [5]. These initial frequency chirps compress pulses linearly in the transmission fibers in both cases [16]. In the chirp-free DCF allocation case (b), pre-chirping is not required for the optimal transmission, and transmission performance is improved especially in the positive *Dc* lines [7].

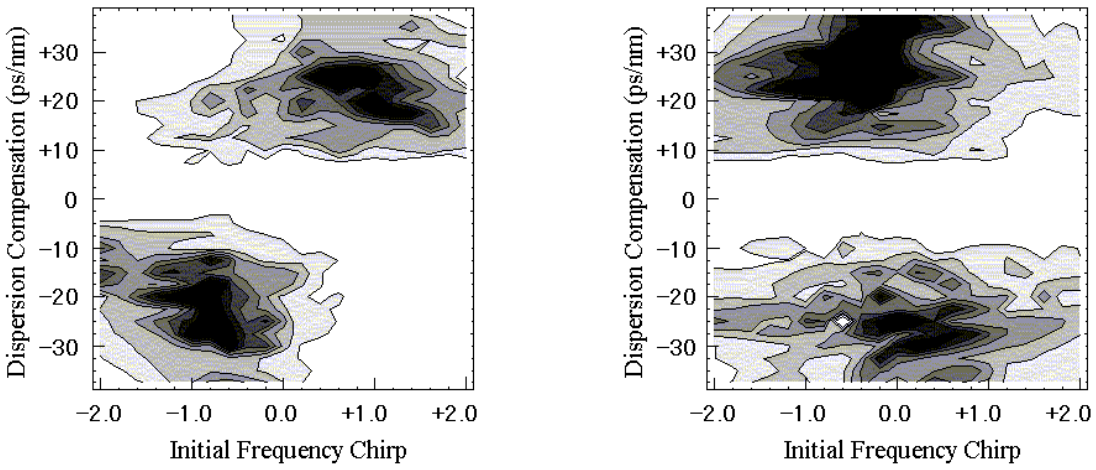

(a) Ordinary DCF allocation

(b) Chirp-free DCF allocation

Figure 12. Q-maps on the *C* – *Dc* planes for (a) Ordinary DCF allocation and (b) Chirp-free DCF allocation. *Pm* = +13 dBm, *Dav* = +0.03 ps/nm/km, *Nc* = 2, *La* = 50 km and *Lt* = 3 Mm.

8. Conclusion

We numerically and experimentally analyzed the optimization method for the dispersion compensated soliton lines. From the simulation results, the optimal dispersion compensation for 40 Gbit/s systems is about ±20 ps/nm, and does not strictly depend on the compensation periods. This result is explained by the interaction mechanism of the dispersion-managed soliton, and simplifies the dispersion design of the transmission lines. We can easily specify the dispersion compensation elements according to the equation (3).

We experimentally evaluated the 40 Gbit/s, 640 km dispersion managed soliton transmission lines using 2-pieces of dispersion compensation fibers. The transmission performance is remarkably improved by the location effect of the dispersion compensation elements. We observed error-free transmission in the wavelength range of 1.2 nm in the chirp-free DCF allocation; 3-times improvement to the ordinary allocation is achieved.

The numerical simulation method using Q-maps is applied to the estimation of the DM-soliton transmissible conditions. The optimal transmission condition shows good agreement with the experimental results, but wavelength margin or power margin is slightly different. By considering the dispersion fluctuation of the transmission fiber, and fiber input power estimation including ASE noise power will improve the accuracy of the numerical simulation.

References

1. Mollenauer, L. F., Evangelides Jr., S. G., and Haus, H. A.: Long-distance soliton propagation using lumped amplifiers and dispersion shifted fiber, *J. Lightwave Technol*. **9**, (1991), pp.194-197.
2. Nakazawa, M., Kubota, H., Suzuki, K., Yamada, E., and Sahara, A.: *Superb characteristics of dispersion-allocated soliton transmission in TDM and WDM systems*, in A. Hasegawa (Ed.), New trends in optical soliton transmission systems, Kluwer Academic Publishers, (1998), pp.197-224.
3. Morita, I., Tanaka, K., Edagawa, N., and Suzuki, M.: 40 Gbit/s single-channel soliton transmission over 10200 km without active inline transmission control, *ECOC'98* (Madrid), **PD**, (1998), pp.49-51.
4. Suzuki, M., Morita, I., Edagawa, N., Yamamoto, S., Taga, H., and Akiba, S.: Reduction of Gordon-Haus timing jitter by periodic dispersion compensation in soliton transmission, *Electron. Lett.* **31**, (1995), pp.2027-2029.
5. Morita, I., Suzuki, M., Edagawa, N., Tanaka, K., Yamamoto, S., and Akiba, S.: Performance improvement by initial phase modulation in 20 Gbit/s soliton-based RZ transmission with periodic dispersion compensation, *Electron. Lett*., **33**, (1997), pp.1021-1022.

6. Jacob, J. M., Golovchenko, E. A., Pilipetskii, A. N., Carter, G. M., and Menyuk, C. R.: Experimental demonstration of soliton transmission over 28 Mm using mostly normal dispersion fiber, *IEEE Photon. Technol. Lett*., **9**, (1997), pp.130-132.
7. Shimoura, K., and Seikai, S.: Two extremely stable conditions of optical soliton transmission in periodic dispersion compensation lines*, IEEE Photon. Technol. Lett*., **11**, (1999), pp.200-202.
8. Yu, T., Golovchenko, E. A., Pilipetskii, A. N., and Menyuk, C. R.: Dispersion-managed soliton interactions in optical fibers, *Optics Lett*., **22**, (1997), pp.793-795.
9. Liang, A., Toda, H., and Hasegawa, A.: High speed optical transmission with dense dispersion managed soliton, *ECOC'99* (Nice), **1**, (1999), pp.386-387.
10. Turitsyn, S. K., Fedoruk, M. P., Doran, N. J., and Forysiak, W.: Optical soliton transmission in fiber lines with short-scale dispersion management, *ECOC'99* (Nice), **1**, (1999), pp.382-383.
11. Anis, H., Berkey, G., Bordogna, G., Cavallari, M., Charbonnier, B., Evans, A., Hardcastle, I., Jones, M., Pettitt, G., Shaw, B., Srikant, V., and Wakefield, J.: Continuous dispersion managed fiber for very high speed soliton systems, *ECOC'99* (Nice), **1**, (1999), pp.230-231.
12. Sahara, A., Kubota, H., and Nakazawa, M.: Q-factor contour mapping for evaluation of optical transmission systems: soliton against NRZ against RZ pulse at zero group velocity dispersion, *Electron. Lett*. **32**, (1996), pp.915-916.
13. Bergano, N. S., Kerfoot, F. W., and Davidson, C. R.: Margin measurements in optical amplifier systems, *IEEE Photon. Technol. Lett.,* **5**, (1993), pp.304-306.
14. Hasegawa, A. and Kodama, Y.: Signal transmission by optical solitons in monomode fiber, *Proceeding of the IEEE*, **69**, (1981), pp.1145-1150.
15. Hasegawa, A. and Kodama, Y.: *Solitons in Optical Communications*, Oxford University Press, (1995), Chap.8.
16. Agrawal, G. P.: *Nonlinear Fiber Optics*, Academic Press, (1995), Chap.3.
17. Sahara, A., Suzuki, K., Kubota, H., Komukai, T., Yamada, E., Imai, T., Tamura, K., and M. Nakazawa, M.: Single channel 40 Gbit/s soliton transmission field experiment over 1000 km in Tokyo metropolitan optical loop network using dispersion compensation, *Electron. Lett*., **34**, (1998), pp.2154-2155.
18. Nielsen, T. N., Stentz, A. J., Hansen, P. B., Chen, Z. J., Vengsarkar, D. S., Strasser, T. A., Rottwitt, K., Park, J. H., Stulz, S., Cabot, S., Feder, K. S., Westbrook, P. S., and Kosinski, S. G.: 1.6 Tb/s (40 x 40 Gb/s) transmission over 4x100 km nonzero-dispersion fiber using hybrid Raman/Erbium-doped inline amplifiers, *ECOC'99* (Nice), **PD2-2**, (1999), pp.26-27.